Energies **2013**, *6*, 282-293; doi:10.3390/en6010282

OPEN ACCESS

energies

ISSN 1996-1073

www.mdpi.com/journal/energies

Article

Long Term Performance Study of a Direct Methanol Fuel Cell Fed with Alcohol Blends

Teresa J. Leo [1,*], Miguel A. Raso [2], Emilio Navarro [3] and Eleuterio Mora [4]

[1] Departmento de Sistemas Oceánicos y Navales, ETSI Navales, Universidad Politécnica de Madrid, Madrid 28040, Spain

[2] Departmento de Química Física I, Facultad de Ciencias Químicas, Universidad Complutense de Madrid, Madrid 28040, Spain; E-Mail: marg@quim.ucm.es

[3] Departmento de Motopropulsión y Termofluidodinámica, ETSI Aeronáuticos, Universidad Politécnica de Madrid, Madrid 28040, Spain; E-Mail: emilio.navarro@upm.es

[4] Departmento de Ciencias Aplicadas a la Ingeniería Naval, ETSI Navales, Universidad Politécnica de Madrid, Madrid 28040, Spain; E-Mail: eleuterio.mora@upm.es

* Author to whom correspondence should be addressed; E-Mail: teresa.leo.mena@upm.es; Tel.: +34-913-367-147; Fax: +34-915-442-149.

Received: 7 November 2012; in revised form: 17 December 2012 / Accepted: 5 January 2013 / Published: 11 January 2013

Abstract: The use of alcohol blends in direct alcohol fuel cells may be a more environmentally friendly and less toxic alternative to the use of methanol alone in direct methanol fuel cells. This paper assesses the behaviour of a direct methanol fuel cell fed with aqueous methanol, aqueous ethanol and aqueous methanol/ethanol blends in a long term experimental study followed by modelling of polarization curves. Fuel cell performance is seen to decrease as the ethanol content rises, and subsequent operation with aqueous methanol only partly reverts this loss of performance. It seems that the difference in the oxidation rate of these alcohols may not be the only factor affecting fuel cell performance.

Keywords: direct alcohol fuel cell (DAFC); mixed alcohol fuel; methanol/ethanol blends; DMFC long term experimental study

Nomenclature:

c	Global alcohol concentration
E	Nernst potential under operating conditions
EtOH	Ethanol

j	Current density
MeOH	Methanol
P	Fixed parameters required by the model
R_{int}	Global resistance times area
V	Output voltage of the fuel cell
y_E	Molar proportion of ethanol in the alcohol mixture
y_M	Molar proportion of methanol in the alcohol mixture

Subscripts

a	Anode, anodic
c	Cathode, cathodic
E	Ethanol
M	Methanol

Greek Letters

α	Charge transfer coefficient
γ	Reaction order
η	Overpotential
η_{act}	Activation overpotential
η_{conc}	Concentration overpotential
η_{ohmic}	Ohmic overpotential

1. Introduction

If polymer electrolyte membrane (PEM) fuel cells are to be a commercial success, their development must be guided by the engineering criteria of effectiveness, economy and user friendliness, among others. Research has concentrated and must continue to concentrate on the three main applications of PEM fuel cells (PEMFC): transport; distributed/stationary; and portable power generation [1–4]. Fast-growing power demand for portable electronic devices has led to an increase in portable PEM fuel cell production, a quarter of which corresponds to direct methanol fuel cell (DMFC) units [1]. Hydrogen has high energy content per weight, makes no environmental impact when reacting with oxygen, allows working at ambient operating conditions in a fuel cell and its electrochemical oxidation rate is high [5,6]. Despite the evident advantages of hydrogen, methanol (MeOH) has the benefit of being liquid under ambient conditions and is not subject to the same storage, transport and distribution issues. MeOH is not violently explosive, although it is however toxic and is not easily produced from renewable sources. Ethanol (EtOH) is another candidate fuel for portable fuel cells that is also liquid in ambient conditions and non-explosive, but it is much less toxic than MeOH and from an ecological viewpoint it is exceptional in that it is a chemical fuel in renewable supply [7,8]. EtOH is furthermore less susceptible

to the "crossover" phenomenon. Despite the lower efficiency of direct ethanol fuel cells (DEFC) due to the poor oxidation kinetics of ethanol, important research has been carried out to overcome the drawbacks of the DEFC [1,9–12]. Then it has been found that whereas PtRu/C electrodes are considered suitable for MeOH, the best binary catalyst for EtOH in an acid environment is PtSn/C. But the question is whether the benefits of MeOH and EtOH can be combined to make an ideal fuel and it is interesting to investigate whether a direct alcohol fuel cell (DAFC) fed with a mixture of these alcohols could satisfy both high performance and low toxicity demands.

This possibility has partly been addressed in two published research papers. The first reports an experimental study of the response of a DMFC when the fuel is changed from MeOH to EtOH [13], finding that the use of EtOH instead of MeOH worsens the cell performance at any given temperature. The second experimental work [14], using alcohol blends to fuel DAFCs, found that fuel cell performance drops significantly even at low EtOH contents in the MeOH/EtOH blends. Focusing on an experimental comparison of catalyst performance, the authors proposed that the main factor explaining the experimental data was the difference in the oxidation rate between both alcohols.

This paper presents a long term study of a DMFC fed with MeOH/EtOH mixtures. The study has three main objectives. The first is to evaluate the fuel/fuel cell behaviour and identify the main experimental problems that arise when alcohol blends are used in different proportions to feed a DMFC. Despite the evident problems with the catalyst, whose optimization should be an important goal, a custom DMFC has been built, activated and then fed with a series of aqueous MeOH/EtOH mixtures with different alcohol ratios. The second objective of this work is to evaluate the long term behaviour of this assembly. After operating with alcohol mixtures, the cell has been repeatedly operated with MeOH solutions in order to check whether the cell performance fully recovers. This process has been carried out up to three consecutive times, thus providing an indication of the long term behaviour of this fuel cell. The third objective is to evaluate the contribution of each of the main variables governing the processes from a macroscopic point of view. Corresponding experimental polarization curves have been recorded and fitted to an analytical model in order to find out whether a reproducible behavior can be identified.

2. Experimental

The custom fuel cell and experimental setup shown in Figure 1, as well as the measurement and control equipment used, have been described elsewhere [13]. The single fuel cell consists of a Membrane Electrode Assembly (MEA) and two metallic bipolar plates fabricated from 316 stainless steel including the reactants distribution channels. To register the polarization curves, *i.e.*, voltage (*V*) *versus* current density (*j*), an experimental setup which allows modifying and controlling the temperature of the testing enclosure where the fuel cell is placed, has been devised an fabricated. During the measurements, fuel and oxidant flow rates, oxidant pressure and fuel cell temperature have been controlled.

2.1. Electrodes

The electrodes, with an active area of 5 cm^2, have been supplied by QuinTech e.K. (Göppingen, Germany). The anode, GDE Freudenberg H2315 I3C1, contains a total PtRu loading of 3 mg cm^{-2} onto GDL Freundenberg H2315 I3C1. The cathode, GDE Freudenberg H2315 T10A, contains a total Pt loading of 3 mg cm^{-2} onto GDL Freudenberg H2315 T10A.

Figure 1. Custom experimental setup.

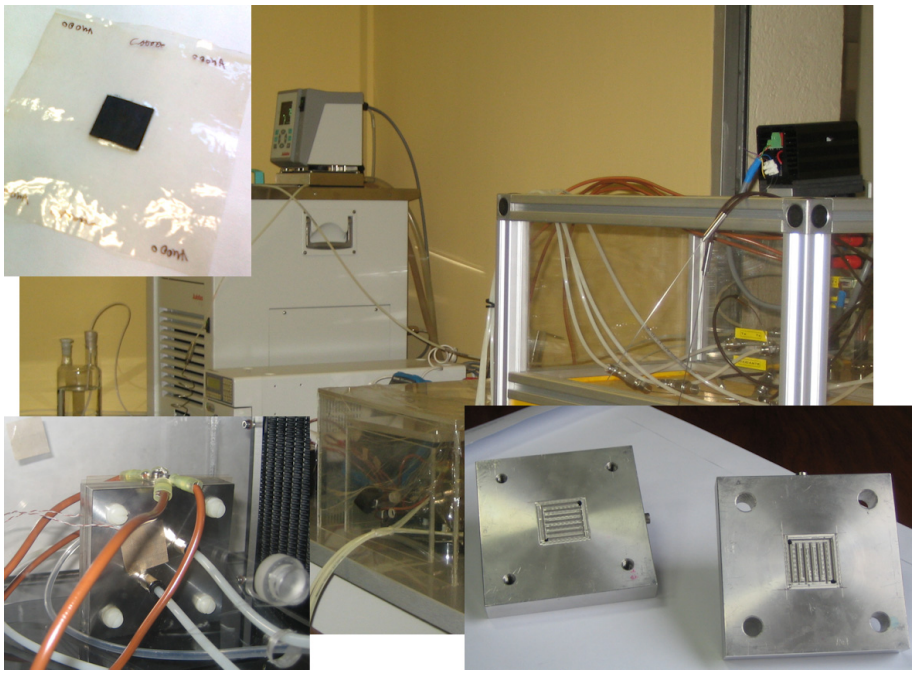

2.2. MEA Preparation

As described previously [13], Nafion® 117 (Dupont, New Castle, DE, USA) has been pre-treated with hydrogen peroxide, 0.5 mol L^{-1} sulphuric acid and distilled water at 80 °C before being sandwiched between the cathode and the anode. After hot pressing at 4 MPa and 135 °C for about 3 min, the homogeneity of the assembly has been checked. Electrochemical activation of the MEA has been conducted before carrying out the set of experiments.

2.3. Experimental Procedure

The two steps described in the following paragraphs have been repeated up to three times, giving rise to three series of experimental data:

1. A series of polarization curves have been recorded for a custom DMFC fuelled by liquid MeOH/EtOH blends in water at a constant total alcohol concentration c of 1 mol L^{-1}. The alcohol blend composition was gradually varied from 1 mol L^{-1} MeOH to 1 mol L^{-1} EtOH using intermediate MeOH/EtOH molar compositions (y_M and y_E, respectively) of 0.90/0.10, 0.70/0.30, 0.50/0.50, 0.30/0.70 and 0.10/0.90. The oxidant was always pure oxygen. The fuel cell temperature was kept constant at 80 °C in every case. Before each test, the cell was preconditioned three times. Polarization curves were recorded three consecutive times for each different fuel composition.
2. The fuel cell was filled with 1 mol L^{-1} aqueous MeOH solution for one week, and then the polarization curve of the fuel cell fed with 1 mol L^{-1} aqueous MeOH was recorded. This step was repeated until the polarization curve remained unchanged.

The total time devoted to the long term experimental study ranged up to 6100 h. The experimental conditions are presented in Table 1.

Table 1. Experimental conditions of measurements.

Parameter	Value
Total alcohol (MeOH/EtOH) concentration (mol L^{-1})	1.0
Alcohol volumetric flow rate (mL min^{-1})	3.0
Oxygen volumetric flow rate (mL min^{-1})	250
Oxygen pressure (bar)	1.0
Temperature (°C)	80

3. Polarization Curve Model for Mixed Alcohol Fuel

3.1. Curve Model

The polarization curve model used was as follows:

$$V = E - \eta_{act,a} - \eta_{act,c} - \eta_{conc,a} - \eta_{conc,c} - \eta_{ohmic} \tag{1}$$

which is an analytical model based on the work of Kulikovsky [15], has been described before [16].

The main equations used to model the polarization curve when the fuel cell is fed with a custom aqueous alcoholic solution are summarized in the following paragraphs.

E stands for the Nernst potential in the operating conditions:

$$E = E^{\circ} + \frac{RT}{z_a F} \ln\left(\frac{c_{CO_2}^{\nu_{CO_2}}}{c_{alc}\, c_{O_2}^{\nu_{O_2}}} \right) \tag{2}$$

ν_{CO_2}, ν_{O_2} and z_a are derived from the reactions' stoichiometry. Solubilities of O_2 and CO_2 in water are taken from [17] to calculate c_{O_2} and c_{CO_2}, respectively. The alcohol concentration in the catalytic layer c_{alc} is calculated as in [18], but multiplied by $(1 - r_c)$ in order to take into account the crossover. The crossover rate r_c is calculated as:

$$r_c = \frac{j_{\text{cross}}}{j_{\text{cross}} + j} \tag{3}$$

where the flux of alcohol through the membrane, expressed in current density units, j_{cross}, is calculated as in [19]:

$$j_{\text{cross}} = \frac{\left(j_{\text{lim}}^{a} - j\right)\left(\beta + n_d\, j/j_w\right)}{j_{\text{lim}}^{a}\left(1 + \beta + n_d\, j/j_w\right)}, \quad \beta = \frac{D_m l_b^a}{D_b^a l_m}, \quad j_w = F D_b^a \frac{w^a}{l_b^a} \tag{4}$$

being w^a the molar concentration of water in the anode channel and j_{lim}^{a}, j_{lim}^{c} stand for the anode and cathode limiting current densities [19], respectively:

$$j_{\text{lim}}^{a} = z_a F \frac{D_b^a c_h^a}{l_b^a}, \quad j_{\text{lim}}^{c} = 4F \frac{D_b^c c_h^c}{l_b^c} \tag{5}$$

In these expressions c_h^a stands for the inlet alcohol concentration, the saturated gaseous oxygen concentration in the inlet flow is calculated as $c_h^c = \left(p_{O_2,in} - p_{sat}(T)\right)\Big/ RT$, l_b^a and l_b^c are the thickness of

the anode and the cathode backing layers, respectively, and D_b^a, D_b^c represent the diffusion coefficient of alcohol and oxygen in their respective backing layers.

The anodic [15,19,20] and cathodic [19,21] activation overvoltages as a function of the exchange current density j_0 and the parameter α are given by:

$$\eta_{act,a} = \frac{RT}{z_a \alpha_a F} \ln \frac{j}{j_{0,a}} \qquad \eta_{act,c} = \frac{RT}{z_c \alpha_c F} \ln \frac{j}{j_{0,c}} \tag{6}$$

The anode exchange current density $j_{0,a}$ can be estimated as a function of the anode reaction order γ_a and the alcohol concentration in the catalytic layer c_{alc}, by means of the following expression derived from [22–24]:

$$j_{0,a} = l_c \left(\frac{c_{alc}}{c_{alc}^{ref}} \right)^{\gamma_a} A_{v,a} j_0^{ref} \tag{7}$$

where $A_{v,a} j_0^{ref}$ represents a reference exchange current density multiplied by the specific surface area on the anode. Values of $j_{0,c}$ have been taken from [21].

The concentration overvoltage is calculated following the expressions given in [15]:

$$\begin{aligned} \eta_{conc,a} &= \frac{RT}{z_a F} \ln \left(\frac{j_{\lim}^a}{j_{\lim}^a - j} (1+\beta) \right) \quad \text{if} \quad j < j_{\lim}^a; \quad \text{otherwise} \quad V = 0 \\ \eta_{conc,c} &= \frac{RT}{z_c F} \ln \left(\frac{j_{\lim}^c}{j_{\lim}^c - j - j_{\text{cross}}} \right) \quad \text{if} \quad j < j_{\lim}^c; \quad \text{otherwise} \quad V = 0 \end{aligned} \tag{8}$$

The ohmic overvoltage is expressed as $\eta_{ohmic} = R_{int} j$, where R_{int} stands for the internal resistance multiplied by the area.

In summary, the model includes a set of fixed parameters taken from the literature, see Table 2, and three fitting parameters that are related to three factors affecting the efficiency of the fuel cell:

- The global anode reaction order, γ_a (chemical kinetics);
- The anode charge transfer coefficient α_a (electrode charge transfer);
- The cell resistance by area R_{int} (global charge transport).

3.2. Mixture Model

This model weights the fixed parameters according to the proportion of each alcohol in the mixture (y_M and y_E), while parameters γ_a, α_a and R_{int} are assumed to be unique (they are not averaged) for each MeOH/EtOH mixture:

$$V = V\left[\left(y_M \vec{P}_M + y_E \vec{P}_E \right), \gamma_a, \alpha_a, R_{int}, j, c \right] \tag{9}$$

where $\vec{P}_M$ and $\vec{P}_E$ stand for all parameters in Table 2, required by the model. Therefore, only γ_a, α_a and R_{int} are fitted to the model in each case, for each aqueous MeOH/EtOH mixture of global alcohol concentration *c*.

Table 2. Assumed parameter values for MeOH and EtOH.

Parameter	MeOH	EtOH
Standard Nernst potential $E°$ (V)	1.214	1.146
Number of electrons considered in the anodic reaction z_a	6	12
Membrane thickness l_m (m)	1.78×10^{-5} [25]	1.78×10^{-5} [25]
Backing layer thickness (anode and cathode) l_b (m)	3.00×10^{-5} [25]	3.00×10^{-5} [25]
Catalyst layer thickness (anode and cathode) l_c (m)	2.0×10^{-6} [26]	2.0×10^{-6} [26]
Cathode transfer α^c coefficient	1 [22,26]	1 [22,26]
Electro-osmotic drag coefficient n_d	3.16 [26]	3.16 [26]
Diffusion coeff. of oxygen in the cathode backing layer D_b^c (m^2 s^{-1})	3.38×10^{-5} [27]	3.38×10^{-5} [27]
Order of reaction (cathode) γ_c	1 [22,26]	1 [22,26]
Anode reference exchange current density multiplied by the specific surface area $A_{v,a} j_0^{ref}$ (A cm^{-3})	$0.100 \times e^{\frac{35570}{R}\left(\frac{1}{353}-\frac{1}{T}\right)}$ [22]	$0.179 \times e^{\frac{39332}{R}\left(\frac{1}{353}-\frac{1}{T}\right)}$ [26]
Cathode exchange current density $j_{0,c}$ (A cm^{-2})	1.87×10^{-8} [21]	1.87×10^{-8} [21]
Diffusion coeff. of alcohol in the anode backing layer D_b^a (m^2 s^{-1})	2.984×10^{-9} [28]	2.984×10^{-9} [28]
Diffusion coeff. of alcohol in the membrane D_m (m^2 s^{-1})	2.148×10^{-9} [20]	2.97×10^{-9} [27]

4. Results

4.1. Experimental Performance of a DMFC Fed with MeOH/EtOH Aqueous Solution Mixtures

Figure 2 shows the experimental polarization and power curves corresponding to the three series of aqueous MeOH/EtOH mixtures recorded in the custom fuel cell fuelled with a 1 mol L^{-1} aqueous alcoholic solution.

Figure 2. (**a**) (Adapted from [29]) Polarization and (**b**) power curves: experimental (bullets) and fitted (lines). ○: first series, □: second series, ◊: third series.

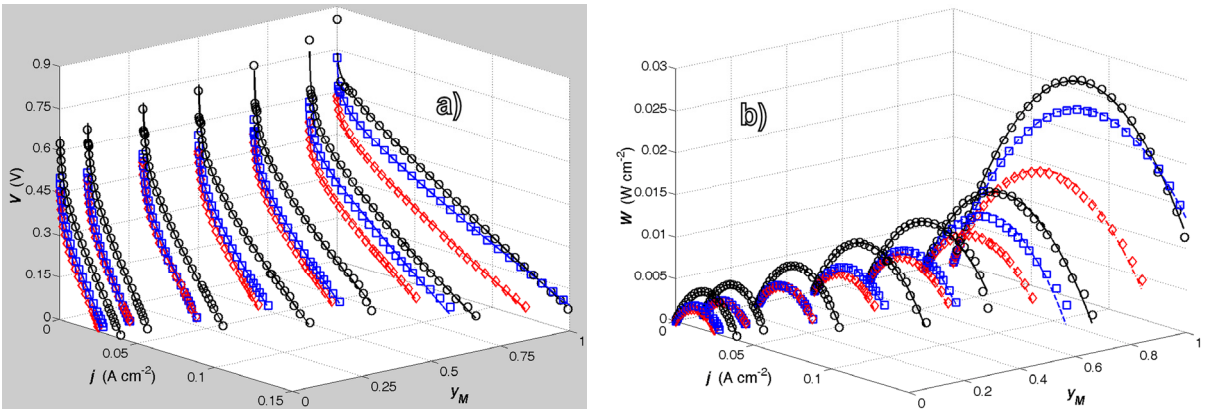

As observed, the fuel cell performance gradually declines from pure MeOH to pure EtOH. Even at a low EtOH concentration, $y_E = 0.1$ and $y_M = 0.9$, EtOH significantly affects the fuel cell behavior. With only a 10% of EtOH in the alcohol mixture the fuel cell maximum power decreases to about half its original value.

4.2. Response of the Fuel Cell to Aqueous MeOH after Being Operated with MeOH/EtOH Mixtures. Fuel Cell Recovery Process

After completing the recording of one series, and before starting the next one, the fuel cell has been operated with 1 mol L^{-1} aqueous MeOH solution until a constant response was obtained. This process, carried out twice, *i.e.*, between the first and second and between the second and third series, is referred to as the "recovery process".

Figure 3a depicts the response of the fuel cell in the first recovery process. As can be seen, its performance successively improves until a constant response is registered. In fact, the polarization curve has practically recovered its initial shape after the third test, but the recovery process has been continued until two successive tests yield the same curve. Although the open circuit voltage *E* (OCV) is lower than the one obtained in the first operation with 1 mol L^{-1} aqueous MeOH, the fuel cell performance at high current density values is recovered.

Figure 3. (**a**) Recovery process after first series; (**b**) Control of end of recovery process: Correct fitting.

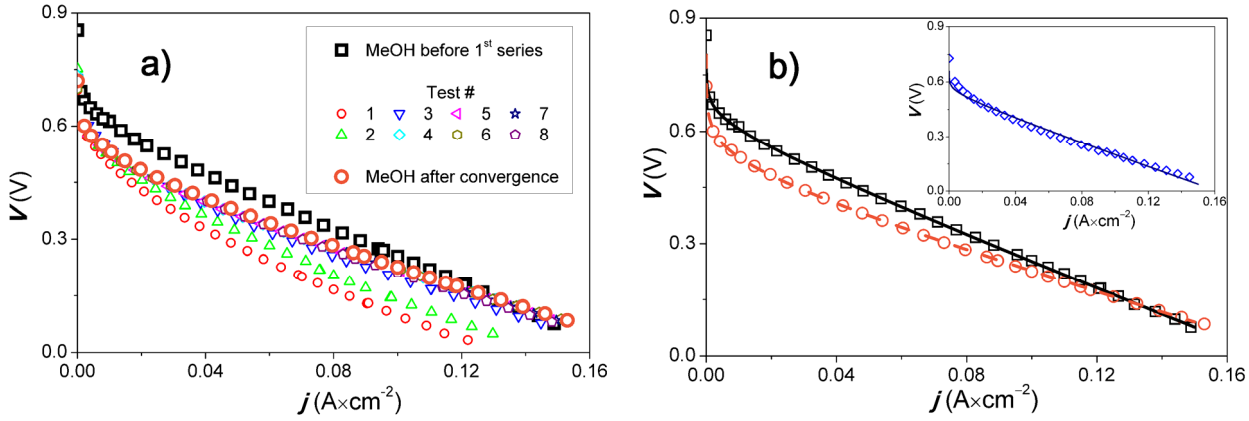

It is important to note, as can be observed in Figure 2, that the fuel cell performance declines when it has been operated with EtOH and the recovery process only partly reverts this loss of performance.

4.3. Curve Fitting

The fitting curves corresponding to the mixture model used, Equation (1), are also plotted in Figure 2. Note the good correlations obtained in all cases.

Figure 3b shows three experimental and fitted polarization curves for the fuel cell operated with 1 mol L^{-1} aqueous MeOH. They correspond to the fuel cell response: (1) before being operated with aqueous EtOH; (2) at an intermediate stage of the recovery process (in the inset); and (3) when no more changes are observed, *i.e.*, when the maximum "recovery" of the fuel cell has been attained. As can be

seen, the experimental data corresponding to situations (1) and (3) is satisfactorily fitted to the proposed model, but this is not valid for the intermediate recovery stage represented by situation (2). In this case the fuel composition does not seem to be defined. This fact supports also the validity of the model.

Figure 4a shows the anode reaction order γ_a obtained along the three series. Its value ends up being practically independent of the mixture composition, reaching the value that corresponds to the first MeOH solution. This suggests that with time the reaction kinetics tends to be independent of the fuel composition.

The resistance by area R_{int} plotted in Figure 4b shows a quite reproducible linear increment with the EtOH content in the mixture but does not depend on the time or the previous history of fuel feeding. Such behavior is also independent of the EtOH proportion in the mixtures previously used. This could point to a membrane proton transfer hindrance caused by EtOH.

Figure 4c shows a power law correlation of the anode charge transfer coefficient α_a data obtained from the three series as a function of the EtOH proportion in the mixture. The power law exponent takes almost the same value (approx. −0.25) for the three series, indicating a common physical origin of the fast decline in α_a with the EtOH proportion. But its value does not return to its original level after the recovery processes, and actually decreases a little more in each successive series. This phenomenon indicates that the difference in the oxidation rate between both alcohols is not the only factor affecting the fuel cell performance and that the electrode charge transfer must be a very important cause of the long term loss of fuel cell performance.

Figure 4. Fitting parameters evolution during long term fuel cell operation (adapted from [29]): (**a**) γ_a, (**b**) R_{int}, (**c**) α_a.

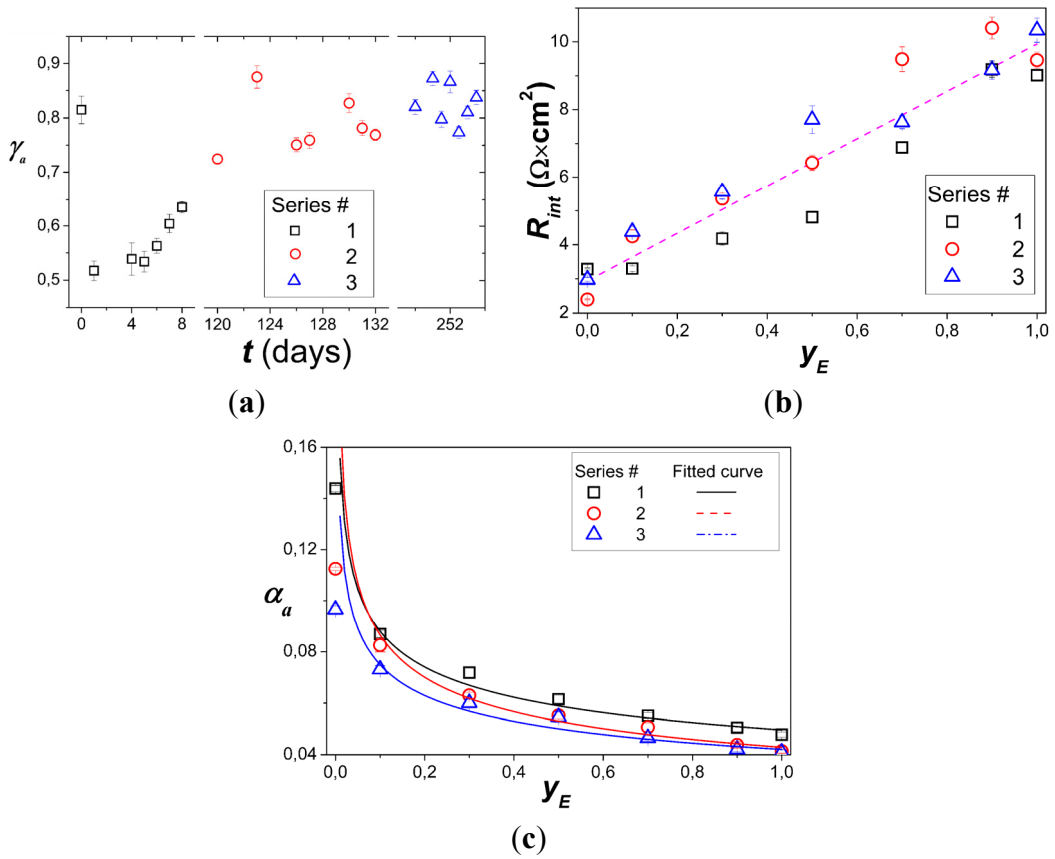

5. Conclusions

With the purpose of investigating the use of direct alcohol fuel cells fed with alcohol blends, this work compares the behaviour of a direct methanol fuel cell fed with aqueous methanol, aqueous ethanol and aqueous methanol/ethanol mixtures by means of a long term experimental study with subsequent modeling of polarization curves.

The following conclusions may be drawn:

- Fuel cell performance declines as the ethanol content in MeOH/EtOH mixture increases.
- The fuel cell recovery process after operation with MeOH/EtOH mixtures only partly reverts the loss of fuel cell performance.
- The anodic global reaction order reaches a value that is independent of the fuel composition (almost recovering its original value) as the fuel cell operation time increases.
- The global charge transport of the fuel cell decreases linearly with the ethanol content in the fuel blend, but is not time-dependent as its original value is restored after each recovery process.
- The anode charge transfer coefficient shows progressive decay with the ethanol proportion in each series, and does not return to its original value after the recovery processes. This points to the fact that the electrode charge transfer must be a very important cause of the long term loss of fuel cell performance.

Acknowledgements

This work has been financially supported by the Spanish Ministerio de Ciencia y Tecnología in the framework of project codes ENE2007-67584-C03-03ALT and ENE2011-28735-C02-02.

References

1. Wang, Y.; Chen, K.S.; Mishler, J.; Cho, S.C.; Adroher, X.C. A review of polymer electrolyte membrane fuel cells: Technology, applications, and needs on fundamental research. *Appl. Energy* **2011**, *88*, 981–1007.
2. Nishimura, A.; Shibuya, K.; Morimoto, A.; Tanaka, S.; Hirota, M.; Nakamura, Y.; Kojima, M.; Narita, M.; Hu, E. Dominant factor and mechanism of coupling phenomena in single cell of polymer electrolyte fuel cell. *Appl. Energy* **2012**, *90*, 73–79.
3. Barelli, L.; Bidini, G.; Gallorini, F.; Ottaviano, A. Dynamic analysis of PEMFC-based CHP systems for domestic application. *Appl. Energy* **2012**, *91*, 13–28.
4. Ahn, S.H.; Choi, I.; Kwon, O.J.; Kim, J.J. One-step co-electrodeposition of Pt–Ru electrocatalysts on carbon paper for direct methanol fuel cell. *Chem. Eng. J.* **2012**, *181–182*, 276–280.
5. Léon, A. *Hydrogen Technology: Mobile and Portable Applications*; Springer-Verlag Berlin-Heidelberg: Berlin, Germany, 2008; pp. 11–150.
6. Rand, D.A.J.; Dell, R.M. *Hydrogen Energy, Challenges and Prospects*; RSC Publishing: Cambridge, UK, 2008; pp. 28–33.
7. Hotza, D.; Diniz da Costa, J.C. Fuel cells development and hydrogen production from renewable resources in Brazil. *Int. J. Hydrog. Energy* **2008**, *33*, 4915–4935.

8. Gnansounou, E. Production and use of lignocellulosic bioethanol in Europe: Current situation and perspectives. *Bioresour. Technol*. **2010**, *101*, 4842–4850.
9. Andreadis, G.; Stergiopoulos, V.; Song, S.; Tsiakaras, P. Direct ethanol fuel cells: The effect of the cell discharge current on the products distribution. *Appl. Catal. B* **2010**, *10*, 157–164.
10. Zhou, W.J.; Zhou, B.; Li, W.Z.; Zhou, Z.H.; Song, S.Q.; Sun, G.Q.; Xin, Q.; Douvartzides, S.; Goula, M.; Tsiakaras, P. Performance comparison of low-temperature direct alcohol fuel cells with different anode catalysts. *J. Power Sources* **2004**, *126*, 16–22.
11. Song, S.; Tsiakaras, P. Recent progress in direct alcohol proton exchange membrane fuel cells (DE-PEMFCs). *Appl. Catal. B Environ.* **2006**, *63*, 187–193.
12. Antolini, E. Catalysts for direct ethanol fuel cells. *J. Power Sources* **2007**, *170*, 1–12.
13. Leo, T.J.; Raso, M.A.; Navarro, E.; Sánchez de la Blanca, E.; Villanueva, M.; Moreno, B. Response of a direct methanol fuel cell to fuel change. *Int. J. Hydrog. Energy* **2010**, *35*, 11642–11648.
14. Wongyao, N.; Therdthianwong, A.; Therdthianwong, S. Performance direct alcohol fuel cells fed with mixed methanol/ethanol solutions. *Energy Convers. Manag.* **2011**, *52*, 2676–2681.
15. Kulikovsky, A.A. *Analytical Modelling of Fuel Cells*, 1st ed.; Elsevier: Amsterdam, The Netherlands, 2010.
16. Leo, T.J.; Raso, M.A.; Navarro, E.; Sánchez de la Blanca, E. Comparative exergy analysis of direct alcohol fuel cells using fuel mixtures. *J. Power Sources* **2011**, *196*, 1178–1183.
17. Lide, D.R. *CRC Handbook of Chemistry and Physics*, 87th ed.; Taylor and Francis: Boca Raton, FL, USA, 2007; pp. 8–84
18. Pramanik, H.; Basu, S. Modeling and experimental validation of overpotentials of a direct ethanol fuel cell. *Chem. Eng. Process. Process Intensif.* **2010**, *49*, 635–642.
19. Kulikovsky, A.A. A method for analysis of DMFC performance curves. *Electrochem. Commun.* **2003**, *5*, 1030–1036.
20. He, Y.; Li, X.; Miao, Z.; Liu, Y. Two-phase modelling of mass transfer characteristics of a direct methanol fuel cell. *Appl. Therm. Eng.* **2009**, *29*, 1998–2008.
21. Parthasarathy, A.; Srinivasan, S.; Appleby, A.J.; Martin, C.R. Temperature dependence of the electrode kinetics of oxygen reduction at the Pt-Nafion® interface—A microelectrode investigation. *J. Electrochem. Soc.* **1992**, *139*, 2530–2537.
22. Xu, C.; Faghri, A. Water transport characteristics in a passive liquid-feed DMFC. *Int. J. Heat Mass Tran.* **2010**, *53*, 1951–1966.
23. Xu, C.; Zhao, T.S.; Yang, W.W. Modeling of water transport through the membrane electrode assembly for direct methanol fuel cells. *J. Power Sources* **2008**, *178*, 291–308.
24. Chen, R.; Zhao, T.S.; Yang, W.W.; Xu, C. Two-dimensional two-phase thermal model for passive direct methanol fuel cell. *J. Power Sources* **2008**, *175*, 276–287.
25. Kulikovsky, A.A. The voltage-current curve of a direct methanol fuel cell: "Exact" and fitting equations. *Electrochem. Commun.* **2002**, *4*, 939–946.
26. Andreadis, G.M.; Podias, A.K.M.; Tsiakaras, P.E. A model-based parametric analysis of a direct ethanol polymer electrolyte membrane fuel cell performance. *J. Power Sources* **2009**, *194*, 397–407.
27. Andreadis, G.M.; Podias, A.K.M.; Tsiakaras, P.E. The effect of the parasitic current on the direct ethanol polymer electrolyte membrane fuel cell operation. *J. Power Sources* **2008**, *181*, 214–227.

28. Arisetty, S.; Advani, S.G.; Prasad, A.K. Methanol diffusion rates through the anode diffusion layer in DMFC from limiting current measurements. *Heat Mass Tran.* **2008**, *44*, 1199–1206.
29. Leo, T.J.; Raso, M.A.; Navarro, E.; Mora, E. Perspectives on the Design and Use of Direct Alcohol Fuel Cells Fed by Alcohol Blends. In *Proceedings of Communication to 6th Dubrovnik Conference on Sustainable Development of Energy Water and Environment Systems*, Dubrovnik, Croatia, 25–29 September 2011.